Analysis of Bistatic Ground Clutter and Applications to Target Plotting

Jan PIDANIC [1], *Karel JURYCA* [1], *Amit Mishra KUMAR* [2]

[1] Dept. of Electrical Engineering, University of Pardubice, Studentská 95, 532 10, Pardubice, Czech Republic
[2] Dept. of Electrical Engineering, University of Cape Town, University Private Bag, Rondebosch, 7701, South Africa

{jan.pidanic, karel.juryca}@upce.cz, amit.mishra@uct.ac.za

Submitted February 8, 2018 / Accepted June 5, 2018

Abstract. *This article presents analysis and parametrization of the bistatic ground clutter which is important from the point of view of the modelling/generating of bistatic clutter, and subsequent developing of the new suppression techniques. The analysis of the bistatic radar has been an active area of research for almost a decade now. The paper includes analysis of bistatic land-clutter trials, run in the Czech Republic, specifically in Pardubice city. First, the theoretical part of bistatic radars and models of bistatic clutter is described. The bistatic clutter is measured by a passive radar system developed by the ERA a.s. company. The analysis of bistatic clutter starts with pre-processing techniques such as antenna virtual rotation and suppression of direct signal. The residuals of the signal are used for bistatic clutter analysis and consequently used for determination of bistatic clutter parameters. These parameters are replicas of individual channels, power of replicas, etc. The output is the development of universal analysis software for bistatic clutter that is used for bistatic clutter generation, mandatory for developing suppression techniques.*

Keywords

Bistatic radar, ground clutter, simulation, measurement, signal processing

1. Introduction

Clutter in radar terminology represents unwanted echoes from the environment, received in electronics systems [1]. Clutter is an unwanted part of the received signal and suppression of clutter is one of the major signal processing stages after digitalization of the received signal [2–4]. The successful suppression of clutter depends on the information about the parameters of the clutter.

There are many classic works on measurement and modelling of radar clutters [5–7]. The body of work on sea clutter modelling is extensive and increasing [8–10]. However, dedicated work on measurement and modelling of ground clutter is not huge [11–13]. And work on bistatic clutter is particularly scarce [14], [15].

In this paper we present our work on measurement and modelling of bistatic ground clutter signal. Our work has two major novelties. First of all, analysis of measured ground clutter is not very much discussed in the open literature. And secondly, we believe this is a good addition to the very small set of works on passive bistatic ground clutter modelling [23], [24].

This paper is organized as follows: description of bistatic clutter, experimental setup, pre-processing for clutter analysis and finally analysis and parametrization of the clutter.

2. Bistatic Clutter Description

An individual echo $s_{R1}(t)$ is described by the formula

$$s_{R1}(t) = a_1 \cdot s_T(t - \tau_1) \quad (1)$$

where a_1 is attenuation constant (amplitude), $s_T(t)$ is transmitted input signal, and τ_1 is time delay of input signal. Clutter can be represented as a summation of the individual environment echoes of transmitted signals by the expression

$$s_R(t) = \sum_{k=1}^{K} a_k \cdot s_T(t - \tau_k) \quad (2)$$

where $k = 1, 2, \ldots, K$ represents summation of k individual echoes, a_k are attenuation constants for echoes, τ_k is time delay of input signal for individual echoes. The amplitude and time delay of individual echo depends on the size of reflected objects, materials of objects, etc.

2.1 Bistatic Radar Clutter

The paper will focus on modelling and generation of bistatic clutter. The bistatic radar [16], [17] is radar which has separated transmitted and received part. The passive radar systems based on the bistatic radars are also known under the term of passive coherent location radar systems

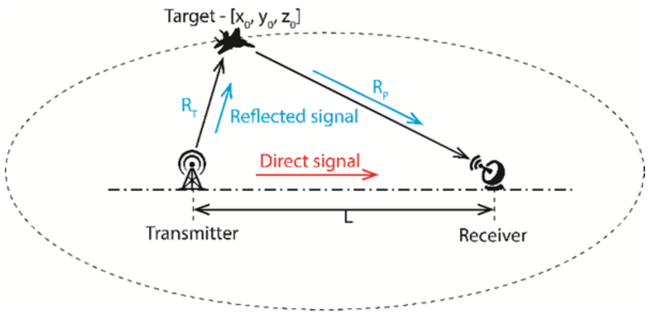

Fig. 1. Geometry of bistatic radar.

(PCL). In the bistatic radar the term 'echo' is not often used, but rather we say replicas of it.

The typical geometry of bistatic radar is shown in Fig. 1. The transmitter and receiver part of the radar is located in the focus of ellipse. The receiver receives signals on the direct path between transmitter-receiver but also receives reflected signals scattered from the environment (bistatic clutter). We can imagine the received reflected signals from environment (clutter) as replicas of direct signal (2).

The main problem in bistatic radar systems is high dynamic range of received signals. The difference in dB between direct signal and reflected signals can achieve about 30–80 dB.

The bistatic radar we have considered uses omnidirectional antenna array with 4–8 elements to cover 360°. Each element of the antenna is used for covering a corresponding azimuth sector. Each element of receiver antenna presents an individual signal channel. The channel where only the direct signal from the transmitter (ideal case) is received is called the reference channel. The other channels are called work channels.

The typical signal processing chain (Fig. 2) in the bistatic radar system is as follows:

(1) Antenna array receive signal

(2) Channel separation (reference and target channels)

(3) Clutter suppression on reference channel and clutter and direct signal suppression on target channels

(4) Computation of Cross Ambiguity function to determination of bistatic range and Doppler speed of targets [18]

(5) Target association [19]

(6) Targets tracking and target plotting

One of the crucial tasks in the signal processing chain in bistatic radar is clutter suppression. In case that clutter suppression technique will be weak or insufficient, then target information is lost in clutter and the radar system may not work properly.

3. Experimental Setup

In this section we shall describe the experimental setup used to collect data which we will be analyzing in this paper.

Specifications of the array antenna (shown in Fig. 3) used in the data-collection drive are as follows. Each antenna element is focused to another frequency band (each element is focused to another transmitter). The antenna parameters are in Tab. 1.

Data are collected after the analog filtration process (3 MHz/3 dB – helical filter) and digitally pre-processed. The processed data is based only on a direct signal from the receiver located in Pardubice and transmitter is located in Černá hora. The parameters of receiver and transmitter position are shown in Tab. 2.

The elevation profile and map of direction between transmitter and receiver are shown in Fig. 5 and 6.

The parameters of the antenna used	
The parameters of transmitter position (detail of antenna in Fig. 3)	
Number of antenna elements [-]	8
Main lobe of each antenna –3 dB [°]	60
Gain of the antenna element [dB]	6
Frequency bandwidth [MHz] (helical filters)	3
Frequency band	VHF

Tab. 1. Antenna parameters.

The parameters of receiver position	
Antenna center coordinates Lat, Lon, Alt [deg, deg, m]	[50.0202777; 15.807777; 240]
Antenna element's boresight azimuth [#1; #2; …; #8]	[24.9026; 69.9026; 114.9026; 159.9026; 204.9026;249.9026; 294.9026; 339.9026]
Azimuth to the transmitter [deg]	[356.20]
The parameters of transmitter position (detail of antenna in Fig. 4)	
Antenna coordinates Lat, Lon, Alt [deg, deg, m]	[50.65250000; 15.741666667; 1343]
Antenna coordinates in 3D coord. system with receiver as origin x; y; z [m; m; m]	[–4676.35; 70341.06; 714.18]
EIRP [kW]	10.64
Carrier frequency [MHz]	88.5
Distance to receiver [m]	70 500
Azimuth position between the transmitter and the receiver on the map (Fig. 6) [deg]	176.20

Tab. 2. The receiver and transmitter azimuth parameters.

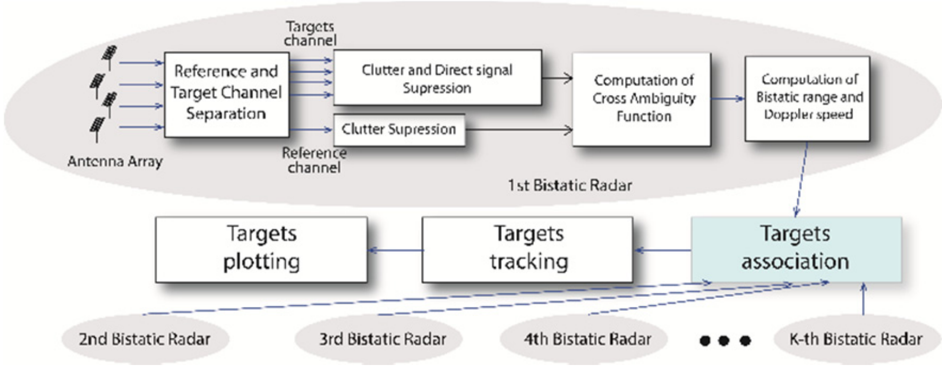

Fig. 2. The signal processing chain of the bistatic radar [20].

Fig. 3. Receiver's antenna [21].

Fig. 4. Transmitter's antenna. 8 dipoles array pointing to 3 directions with 90° step (azimuths 90, 180 and 270°).

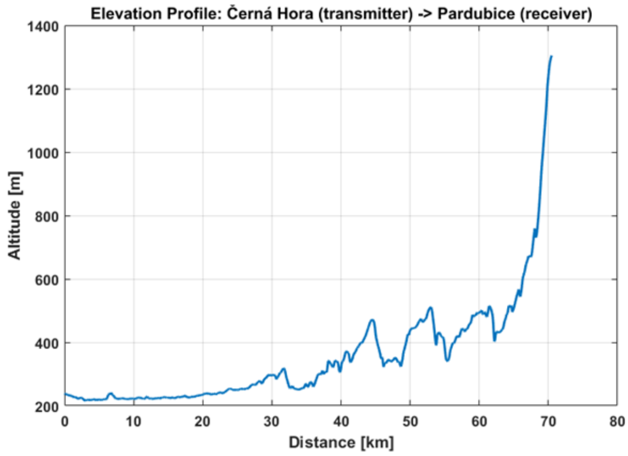

Fig. 5. Elevation profile of the transmitter and receiver.

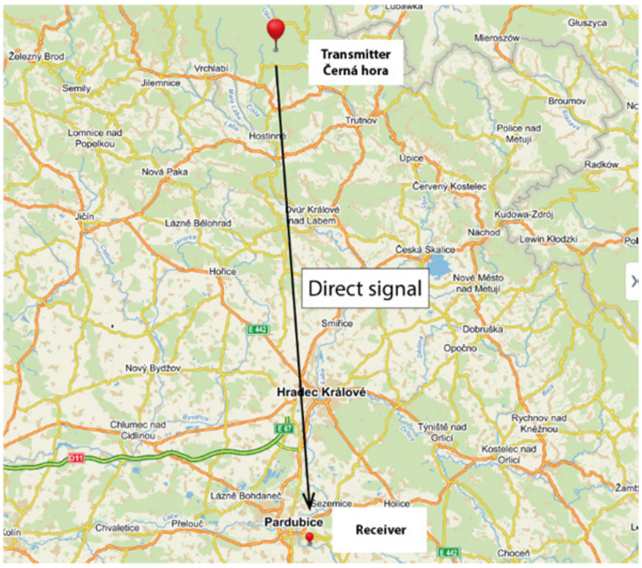

Fig. 6. The direction of the transmitter-receiver [22].

4. Preprocessing for Clutter Analysis

Clutter, like any other type of signal, can be described by signal characteristics. This chapter describes measurement, analysis and extraction of characteristics of the clutter. The clutter was provided by company Era a. s. [21].

The measured signal used for determination of clutter is shown in Tab. 3.

Before clutter analysis it is necessary to preprocess input measured signal with parameters, as stated below. The additional steps are:

(1) The rotation of input signal.

(2) The decimation of input signal.

(3) The suppression of direct signal in work channel.

The parameters of measured data	
Length of signal [s]	1
Number of samples per channel N [-]	293 940
Number of channels M [-]	8
Total number of samples N_T [-]	1 919 520
Sampling frequency f_s [kHz]	240
Carrier frequency f_0 [kHz]	88.5
Size of resolution cell [km]	1.235
The maximal distance of computed replicas d_{max} [km]	100

Tab. 3. The parameters of measured data.

4.1 The Rotation of Input Signal

The receiver antennas have eight elements (Fig. 7). The maximum of radiated power of each antenna element is rotated by 45°. The coverage of this antenna array is 360°.

The input signal received by the antenna array is described by a matrix with eight columns where each column presents one signal channel. The length of each channel is 239 940 rows (number of samples per each channel). The individual channel presents a complex envelope of a signal received on each antenna element. The original rotation of receiver antenna is shown in Fig. 7 (left).

The transmitter is located between antenna element (beam) one and eight. For the best elimination of the direct signal we make a rotation of antenna array of about 22.5° to left. The results after rotation of the antenna array is shown in Fig. 7 (right).

After rotation, antenna element beam 1 (channel 1) is oriented directly to the transmitter Černá hora. Channel 1 can be considered as a reference channel which receives only a direct signal without any other reflections (ideal case). The received power at each channel is normalized to the total received power. The normalized powers for each channel before and after antenna rotation are shown in Fig. 8.

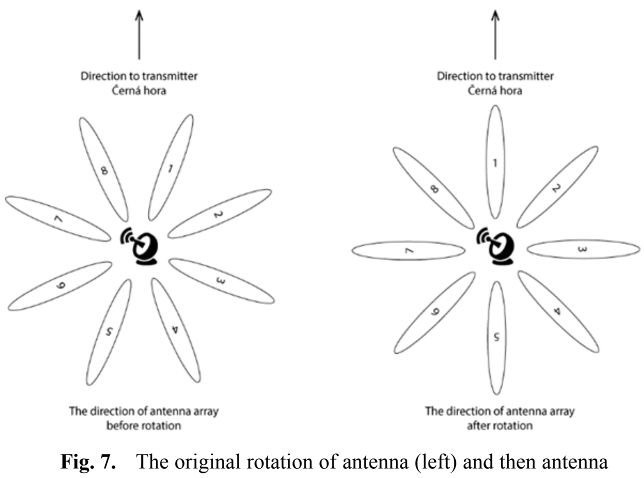

Fig. 7. The original rotation of antenna (left) and then antenna array after rotation –22.5° (right).

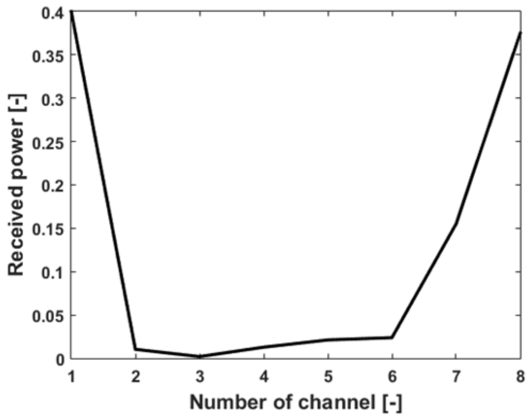

(a)

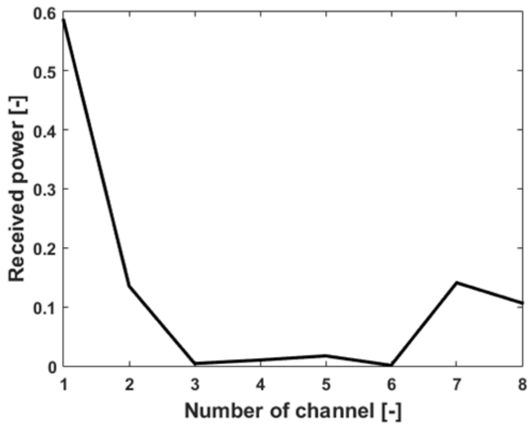

(b)

Fig. 8. Received power at each channel before (a) and after (b) rotation of the antenna.

4.2 The Decimation of Input Signal

The decimation of input signal is necessary due to

(1) High number of samples of input signal. The computation time significantly increases with number of samples.

(2) Requirement of independences between samples. In case of very high sample rate of input signal, the samples will not be independent.

For the clutter analysis we consider decimation factor of two (we take every second sample from the input signal). The total number of samples after decimation is $N_d = 119\,970$.

4.3 The Suppression of Direct Signal in Work Channel

The suppression of a direct signal in the work channel is necessary for approximation of clutter parameters due to high differences between power of direct signal and reflected signals.

In the case that the direct signal is not suppressed, computation of clutter parameters will be inaccurate (special for reflected signals). For the best approximation of clutter parameters, it is necessary to remove the direct signal from all work channels. After suppression of clutter signals we get a signal which contains only reflections from the environment, i.e. clutter. The powers of all reflected signals are closer, from the point of view of signal dynamic. The suppression of a direct signal improves clutter suppression about 30 dB.

The suppression of a direct signal is computed by the formula

$$s_{sm}(n) = s_m(n) - a_m \cdot s_r(n) \tag{3}$$

where $s_m(n)$ is signal in the mth working channel, $s_r(n)$ is direct signal after decimation, a_m is suppression coefficient of direct signal in the mth working channel, $m = 1,\ldots,M$.

The suppression coefficient for each working channel is computed by the formula

$$a_m = \frac{\sum_{n=1}^{N} s_m(n) \cdot s_r(n)}{\sum_{n=1}^{N} s_r^2(n)}. \tag{4}$$

The differences between received power in working channels before and after direct signal suppression are shown in Fig. 9.

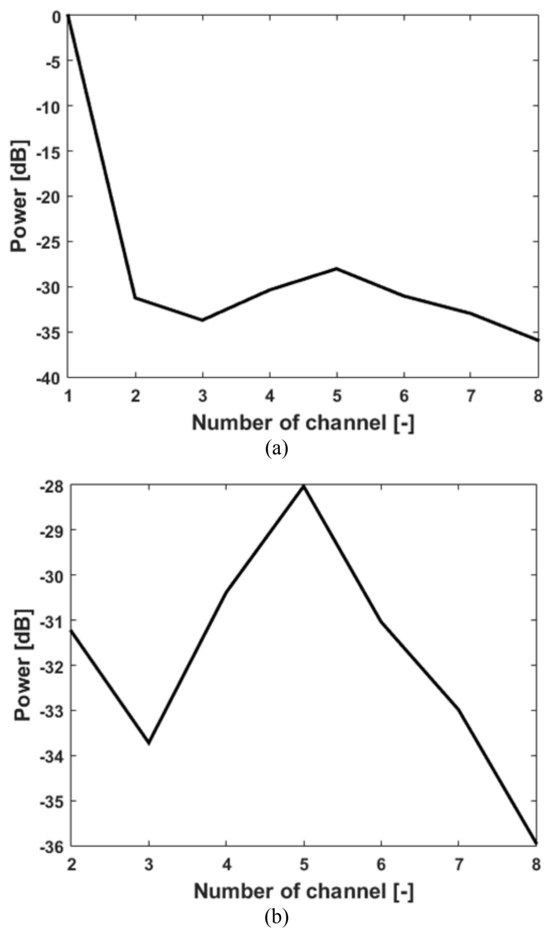

Fig. 9. The received power before (a) and after (b) direct signal suppression.

5. The Clutter Analysis

The clutter is described by replicas of the transmitted input signal from surrounding objects (environment) and can be expressed by power of individual replicas in the specific distances. From the time differences between propagation of direct signal and propagation of each replica, time delays of replicas τ_R or distances ($\Delta R = c\ \tau_R$, $R \in \langle 1 \ldots N_R \rangle$ are computed where R is integer, N_R is number of the replicas. The number of the replicas N_R is computed by the formula

$$N_R = \frac{d_{\max}}{\Delta R} \tag{5}$$

where $d_{\max}$ is the maximal considered distance.

The value of parameter $d_{\max}$ significantly influences the number of replicas and residual power after clutter suppression. The clutter suppression is expressed by residual power in each working channel. The lower value of residual power means that clutter suppression is higher. It was analyzed that the replicas power for $d_{\max} > 100$ km is negligible and for distances higher than 100 km it is not necessary to consider.

The maximum number of replicas for $d_{\max} = 100$ km and $\Delta R = 1.235$ km is

$$N_R = \frac{d_{\max}}{\Delta R} = \lfloor 80.9717 \rfloor = 80. \tag{6}$$

The initial formula for derivation of replicas is

$$\mathbf{Y} = \mathbf{A} \times \mathbf{F} + \mathbf{W} \tag{7}$$

where $\mathbf{Y}$ is the matrix of the received signal, $\mathbf{A}$ is the matrix derived from the reference channel, $\mathbf{F}$ is the matrix of complex amplitudes of the signal replicas, $\mathbf{W}$ is the matrix of white noise.

The replicas $\mathbf{F}$ for individual channels are derived by the method of linear equalization. The process of derivation is

$$\begin{aligned}&\mathbf{A}^{\mathrm{H}} \times \mathbf{Y} = \mathbf{A}^{\mathrm{H}} \times \mathbf{A} \times \mathbf{F} + \mathbf{A}^{\mathrm{H}} \times \mathbf{W},\\ &\left(\mathbf{A}^{\mathrm{H}} \times \mathbf{A}\right)^{-1} \times \mathbf{A}^{\mathrm{H}} \times \mathbf{Y} =\\ &\left(\mathbf{A}^{\mathrm{H}} \times \mathbf{A}\right)^{-1} \times \left(\mathbf{A}^{\mathrm{H}} \times \mathbf{A}\right) \times \mathbf{F} + \left(\mathbf{A}^{\mathrm{H}} \times \mathbf{A}\right)^{-1} \mathbf{A}^{\mathrm{H}} \times \mathbf{W}\end{aligned} \tag{8}$$

where $\mathbf{A}^{\mathrm{H}}$ is the Hermitian transposition of matrix $\mathbf{A}$.

If we consider $\left(\mathbf{A}^{\mathbf{H}} \times \mathbf{A}\right)^{-1} \times \left(\mathbf{A}^{\mathbf{H}} \times \mathbf{A}\right) = 1$ then

$$\left(\mathbf{A}^{\mathrm{H}} \times \mathbf{A}\right)^{-1} \times \mathbf{A}^{\mathrm{H}} \times \mathbf{Y} = \mathbf{F} + \left(\mathbf{A}^{\mathrm{H}} \times \mathbf{A}\right)^{-1} \mathbf{A}^{\mathrm{H}} \times \mathbf{W}. \tag{9}$$

The white noise $\mathbf{W}$ is random, non-correlated noise with Gauss distribution and mean value equal to zero. The estimation of $\hat{\mathbf{F}}$ is

$$\hat{\mathbf{F}} = \left(\mathbf{A}^{\mathrm{H}} \times \mathbf{A}\right)^{-1} \times \mathbf{A}^{\mathrm{H}} \times \mathbf{Y}. \tag{10}$$

The size of matrix $\hat{\mathbf{F}}$ is $[n \times M \times k]$ where n is number of replicas, M is number of channels and k is number of signal sections. The motivation for dividing of input signal into sections is explained in Sec. 5.1. The matrix $\hat{\mathbf{F}}$ for the analyzed input signal has size [80 × 8 × 4].

5.1 The Matrix Y

The matrix **Y** represents the input signal after prerequisite computation. The general size of this signal is $[N \times M]$. Due to reduction of the time computation, the input signal **Y** is divided to four sections ($k = 4$). The size of the new matrix $\mathbf{Y}_N$ is $[N_r \times M \times k]$, where $N_r = N/k$ is the number of samples in each section. In the next formulas original and resized input matrixes are shown:

Original:

$$\mathbf{Y} = \begin{pmatrix} 1,1 & \cdots & 1,M \\ \vdots & \ddots & \vdots \\ N_d,1 & \cdots & N_d,M \end{pmatrix} \quad (11)$$

Resized:

$$\mathbf{Y1} = \begin{pmatrix} 1,1 & \cdots & 1,M \\ \vdots & \ddots & \vdots \\ N_r,1 & \cdots & N_r,1 \end{pmatrix} \quad \mathbf{Y2} = \begin{pmatrix} N_r+1,1 & \cdots & N_r+1,M \\ \vdots & \ddots & \vdots \\ 2N_r,1 & \cdots & 2N_r,1 \end{pmatrix}$$

$$\mathbf{Y3} = \begin{pmatrix} 2N_r+1,1 & \cdots & 2N_r+1,M \\ \vdots & \ddots & \vdots \\ 3N_r,1 & \cdots & 3N_r,1 \end{pmatrix} \quad \mathbf{Y4} = \begin{pmatrix} 3N_r+1,1 & \cdots & 3N_r+1,M \\ \vdots & \ddots & \vdots \\ 4N_r,1 & \cdots & 4N_r,1 \end{pmatrix} \quad (12)$$

5.2 The Matrix A

The matrix **A** contains the section of direct signal from the reference channel (i.e. channel 1 from matrix **Y**). The size of matrix **A** is $[N_r \times M \times k]$. The format of matrix **A** is following:

$$\mathbf{A} = \begin{bmatrix} Y_{n,1} & Y_{n-1,1} & \cdots & Y_{n-(n-2),1} & Y_{n-(n-1),1} \\ Y_{n+1,1} & Y_{n,1} & \cdots & Y_{n-(n-3),1} & Y_{n-(n-2),1} \\ \vdots & \vdots & \ddots & \vdots & \vdots \\ Y_{n+N_r-1,1} & Y_{n+N_r-2,1} & \cdots & Y_{N_r,1} & Y_{N_r-1,1} \\ Y_{n+N_r,1} & Y_{n+N_r-1,1} & \cdots & Y_{N_r+1,1} & Y_{N_r,1} \end{bmatrix}. \quad (13)$$

The samples 1 up to N_r from channel 1 of matrix **Y** are stored in the first row of matrix **A** in reverse order. The samples 2 up to $N_r + 1$ from channel 1 of matrix **Y** are stored in the second row of matrix **A** in reverse order, and so on until the last row.

5.3 The Computation of Replicas for Individual Channels

The computed replicas in the reference (direct) channel are computed for all signal intervals and afterwards are averaged (Fig. 10). The reference channel should contain only one direct signal in the ideal case. In the real situation, it also consists of reflected signals (replicas). The replicas in the reference channel should be neglected due to the fact that replicas power is lower-order in comparison to the power of the direct signal.

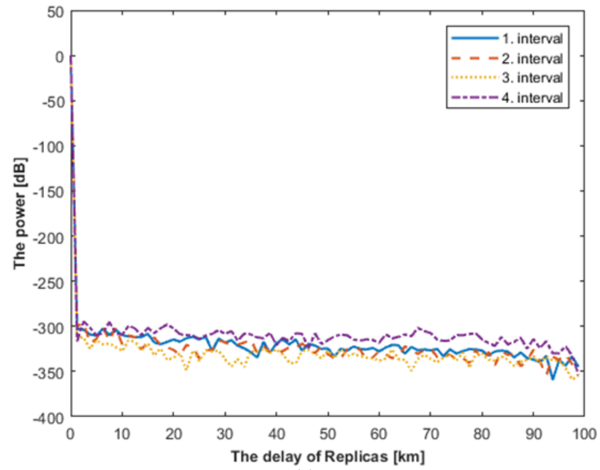

(a)

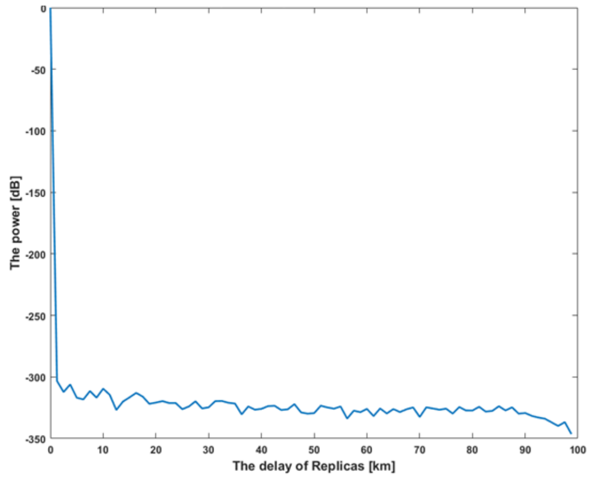

(b)

Fig. 10. (a) The power of the replicas in the reference channel for the individual signal interval. (b) The averaged power of the replicas in the reference channel.

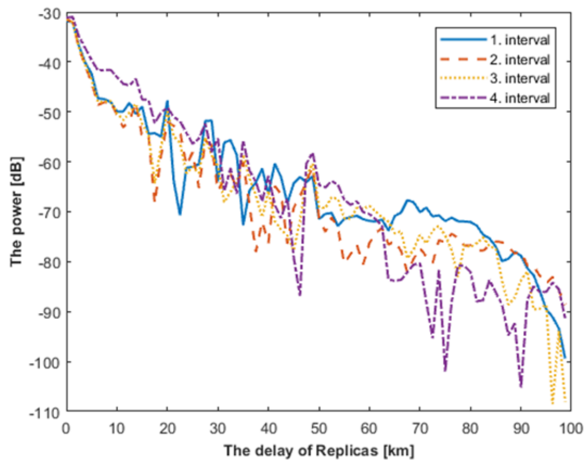

Fig. 11a. The power of the replicas in the second channel for the individual signal intervals.

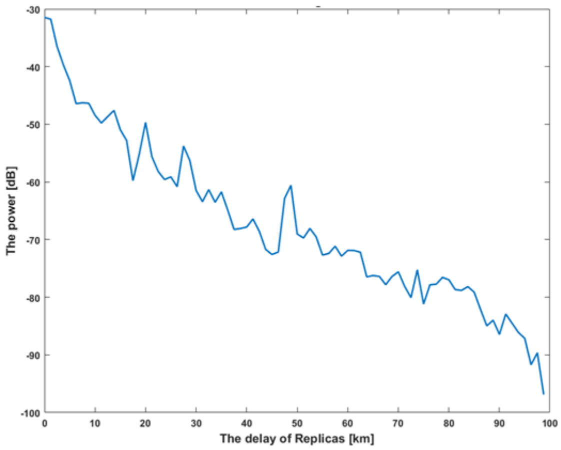

Fig. 11b. The averaged power of the replicas in the working channel 2.

The computed replicas for working channel 2 are shown in Fig. 11. The replicas for distances 0–50 km have similar waveform for all signal intervals. The significant difference between computed replicas occurs for distances 50 km up to 100 km. The causes of these differences are:

- The received signal from the distances 50–100 km is poor (weak).
- The corruption of the received signal by noise.
- The multipath propagation of the signal.

The individual intervals (Fig. 11a) are averaged to the elimination of the differences. The elimination of these differences also simplifies of the bistatic clutter modelling.

5.4 The Residual Power of the Signals

The residual signal is the remaining signal after the clutter suppression. In the ideal case the residual signal should contain only noise and reflection from the targets. The residual signal for the individual channels is computed by the formula

$$\mathbf{Z} = |\mathbf{Y} - \mathbf{A} \times \mathbf{F}| \qquad (14)$$

where **Z** is the matrix with the residual signals for working channels.

The efficiency of the clutter suppression is expressed by the level of the residual signals in the individual working channels. The lower the level of the residual power is, the better is the clutter suppression. The residual power of the working channel 2 for the signal intervals is shown in Fig. 12a. Fig. 12b shows averaged power of the residual signal for channel 2. The residual power of the same channel at distance 50 km is similar to residual power for 100 km.

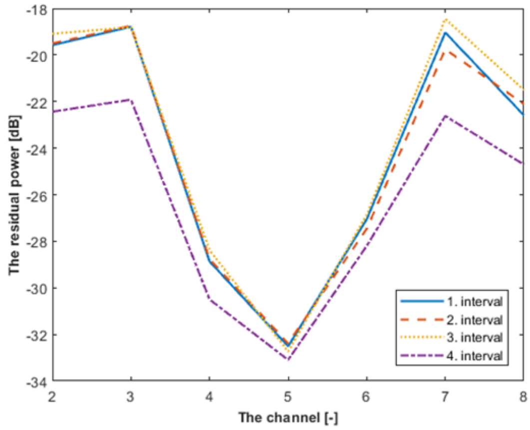

(a)

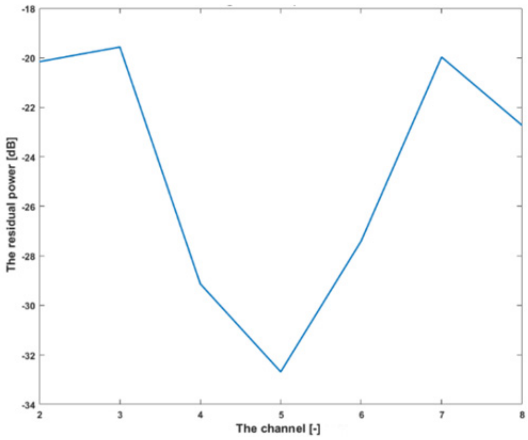

(b)

Fig. 12. (a) The power of the residual signal in the working channel 2 for the individual signal interval at the distance 100 km. (b) The averaged power of the residual signal in the working channel 2 at distance 100 km.

6. Conclusion

The paper presents analysis of bistatic ground clutter measured by a passive radar system from ERA a.s. company. The paper starts with the brief description of the bistatic clutter model and description of bistatic radar systems. The paper continues with description of the setup experiment that includes position of receiver and FM transmitter. The transmitter is located in the mountains in the Czech Republic (Černá hora). The other description is an elevation profile between the transmitter and receiver which significantly influences the power characteristics of reflected bistatic clutter. The pre-processing of gathered data is necessary for parameterization of bistatic clutter. The pre-processing includes virtual rotation of the antenna, suppression of the direct signal and decimation of the signal. The rest of the paper focuses on analysis of bistatic clutter, based on determination of the number of replicas considered in the reflected signal, replica power, etc. The work presents the first step in analysis. Future steps will involve statistical analysis of different measured data for different experimental setups (different position of the receiver, the distance between receiver-transmitter, etc.) and determination of parameters of bistatic clutter. The parametrization will be used for developing of a bistatic clutter generator that will be used for development and validation of clutter suppression techniques. The usage of the generator will be effective from the point of view of time and money compared to measurement of bistatic clutter with a real system under the different setup experiment.

Acknowledgments

The research was supported by the Internal Grant Agency of University of Pardubice, the project No. SGSFEI 2018. The paper is based on a diploma thesis by Jan Pulpan and mentor Jan Pidanic.

References

[1] BEZOUŠEK, P., ŠEDIVÝ, P. *Radar Technology.* 1st ed. Prague (CR): Vydavatelství ČVUT, 2004. 217 p. ISBN 80-010-3036-9 (in Czech)

[2] BARRIE BILLINGSLEY, J. *Low-Angle Radar Land Clutter: Measurements and Empirical Models.* Stevenage, UK: Institution of Electrical Engineers, 2002, 703 p. ISBN 978-1891121166

[3] SEKINE, M., MAO, Y. *Weibull Radar Clutter.* London, UK: P. Peregrinus Ltd., 1990. ISBN 0863411916

[4] CHERNIAKOV, M. *Bistatic Radar: Emerging Technology.* Hoboken, NJ: J. Wiley, 2008. ISBN 978-0470026311

[5] LARSON, R., MAFFETT, A., HEIMILLER, R., et al. Bistatic clutter measurements. *IEEE Transactions on Antennas and Propagation*, 1978, vol. 26, no. 6, p. 801–804. DOI: 10.1109/TAP.1978.1141947

[6] MCLAUGHLIN, D. J., BOLTNIEW, E., RAGHAVAN, R. S., et al. Crosspolarised bistatic clutter measurements. *Electronics Letters*, 1995, vol. 31, no. 6, p. 490–491. DOI: 10.1049/el:19950323

[7] MATKIN, B. L., MULLINS, J. H., FERSTER, T. J. Bistatic reflectivity measurements on various terrains at X, Ku, Ka and W-band frequencies. In *Proceedings of the 2002 IEEE Radar Conference*. Long Beach (CA, USA), 2002, p. 266–271. DOI: 10.1109/NRC.2002.999730

[8] WATTS, S., WICKS, D. C. Empirical models for detection prediction in K-distribution radar sea clutter. In *IEEE International Conference on Radar*. Arlington (VA, USA), 1990, p. 189–194. DOI: 10.1109/RADAR.1990.201160

[9] WATTS, S. A new method for the simulation of coherent sea clutter. In *2011 IEEE RadarCon (RADAR*). Kansas City (MO, USA), 2011, p. 052–057. DOI: 10.1109/RADAR.2011.5960498

[10] WARD, K.D., TOUGH, R. J. A. Modelling radar sea clutter in the littoral. In *IET Seminar on Radar Clutter Modelling*. London (UK), 2008, p. 25–31. DOI: 10.1049/ic:20080146

[11] ZHANA, W. H., LI, Z. Q. Modeling and simulation of ground clutter in the improvement factor test. In *The 6th IEEE Joint International Information Technology and Artificial Intelligence Conference*. Chongqing (China), 2011, p. 250–253. DOI: 10.1109/ITAIC.2011.6030322

[12] LI, SHASHA The study of radar ground clutter simulation based on DEM. In *IEEE International Conference on Information and Automation (ICIA)*. Yinchuan (China), 2013, p. 258–262. DOI: 10.1109/ICInfA.2013.6720306

[13] LE HELLARD, D., HENRY, J. P., AGNESINA, E., et al. Ground clutter simulation for surface-based radars. In *Proceedings of the International Radar Conference.* Alexandria (VA, USA), 1995, p. 579–582. DOI: 10.1109/RADAR.1995.522612

[14] OYEDOKUN, T., INGGS, M. Design and evaluation of a sea clutter simulator. In *IEEE International Geoscience and Remote Sensing Symposium*. Vancouver (Canada), 2011, p. 2089–2092. DOI: 10.1109/IGARSS.2011.6049576

[15] INGGS, M., GRIFFITHS, H., FIORANELLI, F., et al. Multistatic radar: System requirements and experimental validation. In *International Radar Conference*. Lille (France), 2014, p. 1–6. DOI: 10.1109/RADAR.2014.7060435

[16] WILLIS, N. J. *Bistatic Radar.* Boston: Artech House, 1991, 329 p. ISBN 978-0890064276

[17] CHERNIAKOV, M. *Bistatic Radar: Principles and Practice.* Chichester (UK): John Wiley, 2007. ISBN 978-0470026304

[18] PIDANIC, J., NEMEC, Z., DOLECEK, R., et al. Computing of bistatic cross-ambiguity function on GPU. In *IEEE International Symposium on Industrial Electronics*. Taipei (Taiwan), 2013, p. 1–5. DOI: 10.1109/ISIE.2013.6563754

[19] PIDANIC, J., SHEJBAL, T., NEMEC, Z., et al. An optimization of a PHD function for association of targets on multistatic radar. In *RADAR Conference 2014*. Cincinnati (OH, USA), 2014, p. 1084–1089. DOI: 10.1109/RADAR.2014.6875756

[20] PIDANIC, J., SHEJBAL, T., NEMEC, Z., et al. Advanced targets association based on GPU computation of PHD function. In *International Conference on Advanced Computer Science and Information Systems (ICACSIS).* Depok (Indonesia), 2015, p. 13–22. DOI: 10.1109/ICACSIS.2015.7415197

[21] ERA, a. s [Online] Cited 2015-09-15. Available at: http://www.era.cz

[22] MAPY [Online] Cited 2016-05-18. Available at: https://mapy.cz.

[23] PALAMA, R, GRECO, M. S., STINCO, P., et al. Statistical analysis of bistatic and monostatic sea clutter. *IEEE Transactions on Aerospace and Electronic Systems*, 2015, vol. 51, no. 4, p. 3036–3054. DOI: 10.1109/TAES.2015.140438

[24] BROWN, J., WOODBRIDGE, K., STOVE, A., et al. VHF airborne passive bistatic radar ground clutter investigation. In *IET International Conference on Radar Systems (Radar 2012*). Glasgow (UK), 2012, p. 1–5. DOI: 10.1049/cp.2012.1684

About the Authors …

Jan PIDANIC was born in 1979. He received his M.Sc. in 2005 and Ph.D. in 2012 from the University of Pardubice. His research interests (more than 10 years) include signal processing in passive radar systems, bistatic radars, clutter modelling and optimization of signal processing algorithms with parallel processing techniques.

Karel JURYCA was born in 1989. He received his M.Sc. in 2016 from the University of Pardubice. His main research interests are signal processing in primary radars system and passive radar systems.

Amit Kumar MISHRA has an academic career spanning over more than 10 years, most of which he has spent working in the domain of radar system engineering and signal processing. He has worked in IIT Guwahati, Australian National University before joining the University of Cape Town where he is currently an Associate Professor. He has published 28 journal papers in reputed journals, more than 150 conference papers and has co-authored two books (published by Springer). He is also an applicant/co-applicant in 8 patents. He has successfully supervised three PhD students and is currently a Senior Member of IEEE. His current interests include radar system design, engineering design and cognitive engineering.